Massive black hole binary eccentricity in rotating stellar systems

Alberto Sesana[1], Alessia Gualandris[2] and Massimo Dotti[2,3]

[1] *Albert Einstein Institut, Am Mühlenberg 1, Golm, D-14476, Germany.*
[2] *Max-Planck Institut für Astrophysik, Karl-Schwarzschild-Str. 1, D-85741 Garching, Germany*
[3] *Dipartimento di Fisica G. Occhialini, Università degli Studi di Milano Bicocca, Piazza della Scienza 3, 20126 Milano, Italy*

20 January 2013

ABSTRACT
In this letter we study the eccentricity evolution of a massive black hole (MBH) binary (MBHB) embedded in a rotating stellar cusp. Following the observation that stars on counter-rotating (with respect to the MBHB) orbits extract angular momentum from the binary more efficiently then their co-rotating counterparts, the eccentricity evolution of the MBHB must depend on the degree of co-rotation (counter-rotation) of the surrounding stellar distribution. Using an hybrid scheme that couples numerical three-body scatterings to an analytical formalism for the cusp-binary interaction, we verify this hypothesis by evolving the MBHB in spherically symmetric cusps with different fractions $\mathcal{F}$ of co-rotating stars. Consistently with previous works, binaries in isotropic cusps ($\mathcal{F} = 0.5$) tend to increase their eccentricity, and when $\mathcal{F}$ approaches zero (counter-rotating cusps) the eccentricity rapidly increases to almost unity. Conversely, binaries in cusps with a significant degree of co-rotation ($\mathcal{F} > 0.7$) tend to become less and less eccentric, circularising quite quickly for $\mathcal{F}$ approaching unity. Direct N-body integrations performed to test the theory, corroborate the results of the hybrid scheme, at least at a qualitative level. We discuss quantitative differences, ascribing their origin to the oversimplified nature of the hybrid approach.

Key words: black hole physics – methods: numerical – stellar dynamics

1 INTRODUCTION

Since their theoretical prediction in the early 80's (Begelman, Blandford & Rees 1980), massive black hole (MBH) binaries (MBHBs) forming in galactic nuclei following galaxy mergers, have been the main focus of many dynamical studies. In the context of the hierarchical formation of galactic structures (White & Rees 1978) and the MBHs residing at their center, bound MBH binaries forming at parsec scales have to get rid of their orbital energy to reach the point where gravitational waves (GW) emission becomes efficient enough to drive their final coalescence. This is known as the 'last parsec problem' (Milosavljevic & Merritt 2001). Interactions with ambient stars, abundant in dense nuclei, might provide the physical source of energy extraction by means of the slingshot mechanism. That is, in a strong three-body encounter, the light intruder star is ejected at infinity carrying away part of the orbital energy and angular momentum of the massive binary (Mikkola & Valtonen 1992). In the last two decades several analytical and numerical works (Quinlan 1996; Milosavljevic & Merritt 2001; Hemsendorf, Sigurdsson & Spurzem 2002; Milosavljevic & Merritt 2003; Merritt & Poon 2004; Makino & Funato 2004; Baumgardt, Gualandris & Portegies Zwart 2006; Berczik et al. 2006; Merritt & Szell 2006; Merritt, Mikkola & Szell 2007; Matsubayashi, Makino & Ebisuzaki 2007; Sesana et al. 2008; Berentzen et al. 2009; Amaro-Seoane et al. 2010; Sesana 2010) have been devoted to the study of MBHB dynamics in galactic nuclei, the major focus being the evolution of the binary semi-major axis to overcome the 'last parsec problem'. Most of these works also report on the MBHB eccentricity evolution (which is in general more difficult to track and much more affected by numerical noise in N-body simulations), often observing a net increase during the hardening process (see Sesana 2010, for a detailed discussion). This is of particular importance because (i) GW emission efficiency is a strong function of the eccentricity of the system (with eccentric binaries coalescing much faster) and (ii) even a small surviving eccentricity in the GW detection bands will be easily detectable (Porter & Sesana 2010), possibly giving us clues about the binary evolution. Interestingly, the vast majority of the cited papers (with the notable exception of

Berczik et al. 2006; Amaro-Seoane et al. 2010) considered the MBHB evolution in non-rotating stellar systems. There are, however, three good reasons for considering rotating stellar distributions:

(i) observationally, classical galaxy bulges often show some degree of net rotation (see, e.g. Gadotti 2011), and pseudobulges are mainly rotationally supported (e.g. Kormendy, Bender & Cornell 2001). A net rotation is also observed in the central region the Milky Way (Genzel et al. 1996; Schödel, Merritt & Eckart 2009).

(ii) MBHBs formed during galaxy mergers are embedded in the remnant of the fusion of two galactic nuclei. Even assuming that the two nuclei originally had no spin, the orbital angular momentum associated with the merger will form a rotating system (Milosavljevic & Merritt 2001).

(iii) As noted by Iwasawa et al. (2010), counter-rotating stars are much more effective in extracting angular momentum from the MBHB. We therefore expect the MBHB eccentricity to evolve differently depending on the degree of co(counter)-rotation of the surrounding stellar distributions.

In this letter, we study the eccentricity evolution of a MBHB with a small mass ratio (we consider $q \equiv M_2/M_1 = 1/81$) in stellar cusps with different degrees of rotation (from purely co-rotating to purely counter-rotating cusps). We apply the hybrid formalism developed by Sesana et al. (2008, hereafter SHM08) that couples numerical three-body scatterings to an analytical description of the cusp-binary interaction. Given the several simplifying assumptions adopted in the hybrid model that may lead to spurious results when it comes to a delicate quantity like the binary eccentricity, we also performed calibrated direct N-body integrations of the binary-cusp system by means of the direct summation N-body code ϕGRAPE (Harfst et al. 2007). The letter is organized as follows. In Section 2 we present a simple analytical argument to explain the different behaviours of co-rotating and counter-rotating stars interacting with the MBHBs, and we verify it with the support of calibrated three-body experiments. In Section 3 we describe the hybrid and N-body models used to integrate the joint MBHB-cusp evolution. We present the results of the two methods, discussing similarities and differences in Section 4, and we conclude with some final remarks in Section 5.

2 ANALYTICAL BACKGROUND AND THREE BODY SCATTERING

In this section we discuss a simple argument to illustrate the different behaviour of co-rotating and counter-rotating stars in the star-binary interaction. For the sake of simplicity, we focus on a ideal coplanar case. A comprehensive analytical model will be presented in a follow up paper. We consider a system consisting of: (i) a binary with total mass $M = M_1 + M_2$ ($M_2 \ll M_1$), semi-major axis a and eccentricity e, with initial energy $\mathcal{E} = -GM_1M_2/(2a)$ and angular momentum $\mathcal{L} = \mathcal{L}_z = \mu\sqrt{GMa(1 - e^2)}$ (where $\mu = M_1M_2/M$) aligned along the positive z axis; (ii) a star either co-rotating or counter-rotating with the binary , with $m_* \ll M_2$, in Keplerian orbit around M_1 with semi-major axis $a_* \approx a$ and eccentricity $e_* \approx e$. The star is characterized by an initial energy $\mathcal{E}_* \approx -GM_1m/(2a)$ and an-

gular momentum $\mathcal{L}_* = \mathcal{L}_{*,z} \approx \pm m_*\sqrt{GM_1a(1 - e^2)}$ along the z axis ($+$ if co-rotating with the binary, $-$ if counter-rotating). Since $M_2 \ll M_1$, we ignore M_2 in the energy and angular momentum budget of the stars, however such approximation (and the following dissertation) works fairly well also in the case of mildly unequal mass binaries with $q = M_2/M_1 = 1/3$. In any case, in the following we will consider $M_1 \approx M$ (thus, $\mu \approx M_2$). Setting $a_* \approx a$ and $e_* \approx e$ is particularly convenient for making a simple argument, since it cancels out complicated eccentricity dependencies.

The starting point of our model is the definition of the MBHB eccentricity as a function of its energy $\mathcal{E}$ and angular momentum magnitude $\mathcal{L}$:

$$e = \sqrt{1 - \frac{2\mathcal{E}\mathcal{L}^2}{GM^2\mu^3}}. \qquad (1)$$

Differentiation of equation (1) leads to

$$\Delta e = -\frac{(1 - e^2)}{2e}\left(\frac{\Delta\mathcal{E}}{\mathcal{E}} + \frac{2\Delta\mathcal{L}_z}{\mathcal{L}_z}\right) = \frac{(1 - e^2)}{2e}\chi \qquad (2)$$

where χ is defined by the last equality. We note that, being the binary angular momentum oriented along the z axis, and being in general $\Delta\mathcal{L} \ll \mathcal{L}$, the eccentricity evolution depends on $\Delta\mathcal{L}_z$ only. Exchanges of the x and y component of $\mathcal{L}$ will only result in a reorientation of the binary plane, without affecting e. The sign of Δe is therefore defined by the combination χ of the energy and angular momentum variations.

Following the three-body interaction, the star is ejected at infinity. The ejection is usually caused by a close encounter with M_2, that captures and ejects the star. This is known as the *slingshot mechanism*. In general, counter-rotating stars have larger relative velocities with respect to M_2 then co-rotating ones, and therefore their capture and ejection cross sections are much smaller. In the presence of a binary, stars experience an asymmetric potential that allows for variations in the direction of their angular momenta. As shown in Merritt, Gualandris & Mikkola (2009), an eccentric binary exerts a semi-periodic forcing in a direction perpendicular to the orbital plane of the stars. Since the torque acting on the orbital plane of the stars is exerted by the binary, there is a correspondent change in the angular momentum of the secondary, which in turn results in a change in the eccentricity. As a consequence of this torquing mechanism, both initially co-rotating and counter-rotating stars undergo secular evolution, and are ejected when they co-rotate with the binary (Iwasawa et al. 2010). Following this observation, we assume the star's final energy to be negligible (i.e. $\mathcal{E}_{*_f} \approx 0$) and its angular momentum z component to be positive, of the form $\mathcal{L}_{*,z_f} = \eta m_*\sqrt{GM_1a(1 - e^2)}$ (where in general $0 < \eta < 1$). For co-rotating stars we therefore have $\Delta\mathcal{L}_{*,z} = -\Delta\mathcal{L}_z = m_*(\eta - 1)\sqrt{GM_1a(1 - e^2)}$ and $\Delta\mathcal{E}_* = -\Delta\mathcal{E} = GM_1m_*/(2a)$. Substituting in Eq. 2 we obtain

$$\Delta e \propto (2\eta - 3). \qquad (3)$$

The same reasoning applies to the counter-rotating stars, with the exception that now the initial angular momentum is $\mathcal{L}_{*,z} = -m_*\sqrt{GM_1a(1 - e^2)}$, leading to

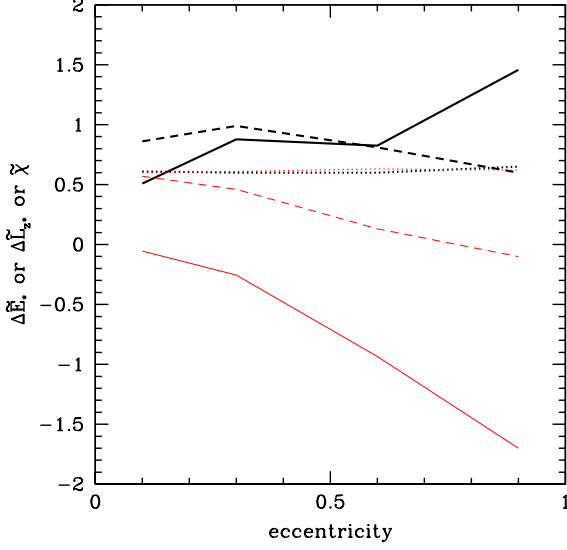$$\Delta e \propto (2\eta + 1). \qquad (4)$$

Figure 1. Average star-binary exchanges in the three body interactions as a function of the MBHB eccentricity. Dashed curves: $\Delta\tilde{\mathcal{L}}_{*,z} = \Delta\mathcal{L}_{*,z}/\mathcal{L}_*^c$ (i.e. the z component of the exchanged stellar angular momentum normalized to the angular momentum of a circular star with the same initial energy); dotted curves: $\Delta\tilde{\mathcal{E}}_*$ (i.e. normalized to the binding energy of a star with $a_* = a$); solid curves $\tilde{\chi} = \chi(M_2/m_*)$. Thick black curves are for counter-rotating stars, thin red curves are for co-rotating stars.

This means that, unless $\eta > 3/2$, the ejection of co-rotating stars decreases e and, conversely, the ejection of counter-rotating stars increases e.

To test this simple heuristic description, we performed four sets of three-body scattering experiments. We considered a binary with $q = 1/81$ and different eccentricities $e = 0.1, 0.3, 0.6, 0.9$. For each binary, we integrated the orbit of 2000 stars with $a_* \approx a$, eccentricity drawn from a thermal distribution $p(e) \propto e$ (to mimic an isotropic distribution), and randomly oriented angular momentum $\mathcal{L}_*$. We stored the energy and angular momentum of each star after the ejection, dividing the stars in two groups: the co-rotating (with $\mathcal{L}_{*,z} > 0$) and the counter-rotating (with $\mathcal{L}_{*,z} < 0$). Figure 1 shows the numerical results of the three-body experiments. The average star-binary energy exchange (dotted lines) is the same for both families and for any binary eccentricity. The angular momentum exchange is instead always much greater for counter-rotating stars, as expected. The practical consequence of this is that the quantity $\chi \propto \Delta e$ is positive for counter-rotating stars and negative for co-rotating stars at any given binary eccentricity. Our simple argument fixes $e_* = e$, to cancel out complications due to eccentricity, and therefore can not catch the Δe dependence on e. However, the main result of our heuristic intuition is corroborated.

3 INTEGRATION OF THE BINARY-STAR SYSTEM

Having understood the different average behaviour of co-rotating and counter-rotating stars, we test here its practical consequences. We follow the evolution of a MBHB in stellar cusps with different degrees of rotation. Integrations are performed both using an hybrid scheme and full direct N-body simulation. In the following, we briefly describe the two techniques.

3.1 The hybrid model

SHM08 constructed an hybrid model for evolving unequal MBHBs in stellar cusps. In short, it works as follows. They integrated 5×10^4 stars in bound orbits around M_1. In the Newtonian limit, the outcome of a scattering depends on $a_*/a \equiv x$, and can be scaled to any absolute value of a. Three-body scattering experiments provide the distributions of the average star-binary energy and angular momentum exchanges $\Delta\mathcal{E}(x)$ $\Delta\mathcal{L}(x)$, together with the bivariate distribution of the ejection times $\mathcal{N}^{\mathrm{ej}}(x, t)$. Such information, obtained numerically, is then coupled to an analytical scheme for the joint evolution of the binary and the surrounding stellar distribution. For the practical integration of the hybrid model, a stellar cusp with density $\rho(r) \propto r^{-\gamma}$, normalized at the binary influence radius to an external isothermal sphere $(\rho(r) = \sigma^2/(2\pi G r^2))$, is assumed. The binary is placed with initial eccentricity e_i at an initial separation a_i where the mass in stars enclosed in its semi-major axis is twice the mass of M_2. In the hybrid model, stars at each x are weighted according to the radial density distribution, a detailed description of the technique is given in SHM08.

The averaging procedure washes out the different behavior of different types of stars having similar values of x. However, here we want to distinguish between co-rotating and counter-rotating stars. We therefore build two sets of distributions $\Delta\mathcal{E}_{p/r}(x)$, $\Delta\mathcal{L}_{p/r}(x)$, $\mathcal{N}^{\mathrm{ej}}_{p/r}(x, t)$, where p (prograde) denotes the average over co-rotating stars only, and r (retrograde) denotes the average over counter-rotating stars. Stellar cusps with different degrees of rotation are constructed by mixing the two distribution as $\mathcal{F}p + (1 - \mathcal{F})r$, where $\mathcal{F}$ is a parameter running from zero to one, describing the fraction of co-rotating stars. We have $\mathcal{F} = 0.5$ for an isotropic cusp while fractions of $\mathcal{F} > 0.5$ (< 0.5) represent cusps with a net degree of co-rotation (counter-rotation) with the binary. Note that, morphologically, the cusp is still spherically symmetric, i.e., this approximation does not take into account any possible axisymmetry or triaxiality induced in the cusp by the rotation. Moreover, being based on three-body scattering experiments, precession effects due to the extended potential of the cusp itself as well as other secular collective effects are ignored.

3.2 N-body simulations

In order to test the hybrid model, we also performed N-body simulations of a MBHB embedded in a power-law stellar cusp and followed its evolution due to interactions with the stars. All the runs were performed with the direct-summation parallel N-body code ϕGRAPE (Harfst et al.
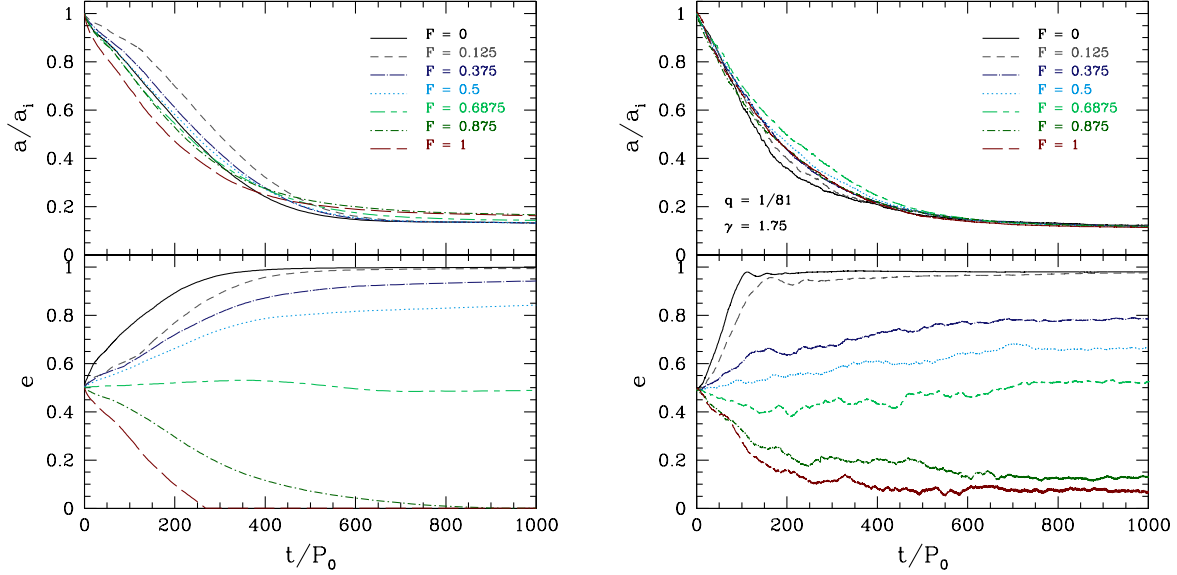
Figure 2. *Left*: semi-major axis (upper panel) and eccentricity evolution (lower panel) of the MBHB according the the hybrid model. Different lines correspond to different fractions of co-rotating stars as labeled in the figure. We assume $q = 1/81$, $\gamma = -7/4$ and $e_i = 0.5$. P_i is the Keplerian orbital period of the binary at a_i. *Right*: same for the direct N-body integrations. Line styles as in the left plot.

2007) on the GPU enabled computers at the Max-Planck Institute for Astrophysics in Garching. The code uses a fourth-order Hermite scheme for the time-integration and can be used in combination with GRAPE or GPU hardware, by means of the `Sapporo` library (Gaburov et al. 2009).

While N-body simulations are computationally much more expensive than three-body integrations and are therefore limited in particle number, they allow to monitor the evolution of the black hole binary under the combined effects of star interactions, Newtonian precession and the Kozai mechanism. Precession of the orbits due to the distributed stellar mass is not taken into account in the hybrid model, but can play a role in the evolution of the binary. Moreover, the cumulative effect of the individual scatterings can significantly change the orientation of the binary orbital plane (Merritt 2002; Gualandris & Merritt 2007), modifying the amount of cusp co-rotation as seen by the binary.

The binary-stellar distribution model was constructed to match the initial set-up used in the hybrid scheme. We considered an unequal-mass binary with primary mass $M_1 = 10^6 \, \mathrm{M_\odot}$, mass ratio $q = 1/81$, initial semi-major axis $a_i = 0.06 \, \mathrm{pc}$ and initial eccentricity $e_i = 0.5$. The stellar cusp follows a Bahcall-Wolf $\rho(r) \sim r^{-7/4}$ profile at distances smaller than $1 \, \mathrm{pc}$, with total mass $M_c \sim 2.5 \times 10^5 \, \mathrm{M_\odot}$ and a mass enclosed in the binary orbit equal to $2M_2$. Because the distribution function adopted for the generation of the initial conditions is approximated, the constructed model is not in exact equilibrium. We therefore let the cusp relax before adding the secondary black hole. During this phase, the system undergoes a small expansion in the outer regions which however does not affect the distance range where the secondary black hole is placed. We use $N = 32768$ for all models which results in a black hole to star mass ratio of $m_*/M_1 = 7.5 \times 10^{-6}$.

In addition to a model with an isotropic distribution of

velocities, we generate models with different fractions of co-rotating stars. These are obtained by reversing the sign of all the velocity components for a random subset of stars, at the time where the second black hole is added. This procedure is effectively equivalent to the mixing procedure $\mathcal{F}p + (1 - \mathcal{F})r$ used in the hybrid scheme.

4 RESULTS

The main results of our experiments are collected in Fig. 2, where the MBHB semi-major axis and eccentricity evolution in cusps with different $\mathcal{F}$ parameter is depicted. In all runs we used $\gamma = -7/4$, $q = 1/81$ and $e_i = 0.5$. The temporal evolution is plotted in units of the initial binary period P_i. The left plot in Fig. 2 shows evolutionary tracks produced by the hybrid integration scheme. The angular momentum of the star is non influential in the energy exchange, hence the orbital decay of the MBHB is hardly affected by the rotation of the cusp. The situation is drastically different in the case of the eccentricity evolution (lower panel). More counter-rotating cusps result in a faster evolution of the binary toward higher eccentricities. The critical fraction defining the transition between eccentricity growth and circularisation, for this particular choice of parameters, is $\mathcal{F} \approx 0.7$. Isotropic cusps ($\mathcal{F} = 0.5$) lead to significant eccentricity growth, as found by SHM08. Results of direct N-body integrations are shown in the right panels of Fig. 2, for the same values of $\mathcal{F}$ used for the hybrid model. As expected, we find that cusps with a larger fraction of stars on co-rotating orbits with respect to the binary tend to circularise the binary while cusps with a larger fraction of stars on counter-rotating orbits tend to increase the binary eccentricity, in agreement with the predictions from the hybrid model. The timescale for the binary decay is also in very good agreement with the

model's results. There are, however, some differences in the N-body results with respect to the model. Firstly, the eccentricity in the N-body integrations does not reach values as low and as high as in the hybrid model. In the fully counter-rotating cusp ($\mathcal{F} = 0$), the eccentricity grows to ~ 0.98 while in the fully co-rotating cusp ($\mathcal{F} = 1$) the eccentricity reaches ~ 0.078. This may be due to the small particle number adopted in the simulations, but also to inaccuracies in the hybrid scheme when interpolations are performed to the eccentricity range boundaries. Also, the model with $\mathcal{F} = 0.5$ shows only a very slow growth in the eccentricity, in contrast with what is found in the hybrid scheme. This may be the result of the suppression of the binary-induced secular evolution of the stars by Newtonian precession related to the extended cusp. As a consequence, counter-rotating stars are less prone to become co-rotating and are less efficient in extracting angular momentum from the MBHB. Lastly, the eccentricity growth in the counter-rotating $\mathcal{F} = 0$ case appears much faster in the N-body results than in the hybrid integration. This is due to the approximations used in the semi-analytic prescription. In the hybrid model, we subtract energy and angular momentum to the binary at the moment of the star ejection. Although this is a good approximation for the energy transfer, it is not for the angular momentum. Stars on counter-rotating orbits secularly subtract angular momentum to the binary to become co-rotating before being ejected. The MBHB eccentricity growth therefore does not occur at the moment of the star ejection (as in our hybrid scheme), but on a shorter timescale, during the star-MBHB interaction. This is reflected in the much faster eccentricity evolution in the counter-rotating N-body runs.

As discussed in Section 3.2, the cumulative torque exerted by the stars changes also the orbital plane of the binary. We find that the orientation changes by $\approx 1 - 4$ degrees on the hardening timescale ($a/\dot{a} \approx 100 P_0$) in all the runs but the two most counter-rotating ($\mathcal{F} = 0, \mathcal{F} = 0.125$). This is in agreement with the change predicted in Eq. 4 of Gualandris & Merritt (2007) for an unequal mass binary. We note that, in the counter-rotating models, the large change in the orbital plane (which results in the binary orbital angular momentum reversal in the $\mathcal{F} = 0$ case) occurs at $t/P_0 > 200$, i.e. *after* the bulk of the orbital evolution. This is because the large eccentricity attained by the binary (following the ejection of a large number of counter-rotating stars) results in a very small angular momentum. In this case, small torques can easily produce a drastic reorientation of the binary plane. This dynamical aspect does not affect our results, but is worth further investigation.

5 FINAL REMARKS

We demonstrate that the degree of rotation of the stellar background surrounding a MBHB determines the eccentricity evolution of the binary. This has already been discussed for wide BH pairs, subject to dynamical friction exerted by a rotating background (Dotti et al. 2007), and in the early evolution of pairing MBHBs in rotating star clusters (Amaro-Seoane et al. 2010). This latter work, in particular, describes the different action of dynamical friction in counter-rotating clusters, and it is somewhat complementary to our paper. Here we highlight for the first time the physical mechanism at work in close binaries evolving through interactions with single stars. We find that, for an unequal mass binary, stellar systems co-rotating with respect to the binary tend to circularise its orbit. On the other hand, if stars have, on average, angular momenta anti-aligned with respect to the binary, a strong increase in the eccentricity is observed.

The dependence of the eccentricity evolution of the binary on the rotation of the stellar background received so far little attention. Rotation can be due to secular evolution or merger events. For equal mass binaries, presumably formed through major galaxy mergers, the MBHs are likely to co-rotate with the nucleus of the remnant, reminiscent of the orbital motion of the parent nuclei. In this case, more circular MBHBs are expected. Very unequal mass binaries could form in situ (see Amaro-Seoane et al. 2007, and references therein), or via galactic minor mergers. In this case, the original rotation of the nucleus of the primary galaxy would be less perturbed by the interaction, possibly resulting in counter-rotating systems, and extremely eccentric binaries. In both equal and unequal cases, the exact eccentricity evolution depends on the degree of rotation and on the slope of the stellar profile. A more detailed analysis is postponed to a future investigation.

REFERENCES

Amaro-Seoane P., Gair J. R., Freitag M., Miller M. C., Mandel I., Cutler C. J. & Babak S., 2007, Class. and Quantum Gravity, 24, 113

Amaro-Seoane P., Eichhorn C., Porter E. K. & Spurzem, R., 2010, MNRAS, 401, 2268

Baumgardt H., Gualandris A. & Portegies Zwart S., 2006, MNRAS, 372, 174

Begelman M. C., Blandford R. D. & Rees M. J., 1980, Nature, 287, 307

Berczik P., Merritt D., Spurzem R. & Bischof H. P., 2006, ApJ, 642, 21

Berentzen I., Preto M., Berczik P., Merritt D. & Spurzem R., 2009, ApJ, 695, 455

Dotti, M., Colpi M., Haardt F. & Mayer L., 2007, MNRAS, 379, 956

Gaburov, E., Harfst, S., & Portegies Zwart, S. 2009, New A, 14, 630

Gadotti D.A., 2011, arXiv:1101.2714

Harfst, S., Gualandris, A., Merritt, D., Spurzem, R., Portegies Zwart, S., & Berczik, P. 2007, New Astronomy, 12, 357

Genzel R., Thatte N., Krabbe A., Kroker H. & Tacconi-Garman L.E., 1996, ApJ, 472, 153

Gualandris A. & Merritt D., 2007, arXiv:0708.3038

Hemsendorf M., Sigurdsson S. & Spurzem R., 2002, ApJ, 581, 1256

Iwasawa M., An S., Matsubayashi T., Funato Y. & Makino J., 2010, arXiv:1011.4017

Kormendy J., Bender R. & Cornell M.E., 2011, Nature, 469, 374

Makino J. & Funato Y., 2004, ApJ, 602, 93

Matsubayashi T., Makino J. & Ebisuzaki T., 2007, ApJ, 656, 879

Merritt D., 2002, ApJ, 568, 998

Merritt D., Gualandris A. & Mikkola S., 2009, ApJ, 693, 35

Merritt D., Mikkola S. & Szell A., 2007, ApJ, 671, 53

Merritt D. & Poon M. Y., 2004, ApJ, 606, 788

Merritt D. & Szell A., 2006, ApJ, 648, 890

Milosavljevic M. & Merritt D., 2001, ApJ, 563, 34

Milosavljevic M. & Merritt D., 2001, ApJ, 596, 860

Mikkola S. & Valtonen M.J., 1992, MNRAS, 259, 115

Perets H. B. & Alexander T., 2008, ApJ, 677, 146

Quinlan G. D., 1996, NewA, 1, 35

Porter E. K. & Sesana A., 2010, arXiv:1005.5296

Sesana, A., Haardt, F., & Madau, P. 2008, ApJ, 686, 432

Sesana A., 2010, ApJ, 719, 851

Schödel R., Merritt D. & Eckart 2009, A&A, 502, 91

White S. D. M. & Rees M. J., 1978, MNRAS, 310, 645